Curr Cardiovasc Imaging Rep (2011) 4:63–76
DOI 10.1007/s12410-010-9058-0

Molecular Imaging of Healing After Myocardial Infarction

Nivedita K. Naresh · Tamar Ben-Mordechai · Jonathan Leor · Frederick H. Epstein

Published online: 20 November 2010

Abstract The progression from acute myocardial infarction (MI) to heart failure continues to be a major cause of morbidity and mortality. Potential new therapies for improved infarct healing such as stem cells, gene therapy, and tissue engineering are being investigated. Noninvasive imaging plays a central role in the evaluation of MI and infarct healing, both clinically and in preclinical research. Traditionally, imaging has been used to assess cardiac structure, function, perfusion, and viability. However, new imaging methods can be used to assess biological processes at the cellular and molecular level. We review molecular imaging techniques for evaluating the biology of infarct healing and repair. Specifically, we cover recent advances in imaging the various phases of MI and infarct healing such as apoptosis, inflammation, angiogenesis, extracellular matrix deposition, and scar formation. Significant progress has been made in preclinical molecular imaging, and future challenges include translation of these methods to clinical practice.

Keywords Molecular imaging · Myocardial infarction · Infarct healing

N. K. Naresh · F. H. Epstein
Department of Biomedical Engineering, University of Virginia,
PO Box 800759, 480 Ray C. Hunt Drive,
Charlottesville, VA 22908, USA

N. K. Naresh
e-mail: nkn3k@virginia.edu

T. Ben-Mordechai · J. Leor
Neufeld Cardiac Research Institute, Tel-Aviv University,
Sheba Medical Center,
Tel-Hashomer 52621, Israel

T. Ben-Mordechai
e-mail: tammybm24@gmail.com

J. Leor
e-mail: leorj@post.tau.ac.il

F. H. Epstein (✉)
Department of Radiology, University of Virginia,
PO Box 800759, 480 Ray C. Hunt Drive,
Charlottesville, VA 22908, USA
e-mail: fredepstein@virginia.edu

Introduction

Myocardial infarction (MI) and associated sequelae such as left ventricular (LV) remodeling and heart failure continue to be a major cause of morbidity and mortality in western countries. Even though nearly all patients that survive an acute MI are now treated with evidence-based medical therapy (β-blockers, statins, aspirin, and angiotensin-converting enzyme inhibitors or angiotensin receptor blockers), approximately 10% to 25% of these patients, depending on age, will be disabled with heart failure within 5 years [1]. In contrast to the established medical therapies that primarily serve to reduce the workload required of the weakened post-MI heart, a number of new experimental therapies aim to improve the infarct healing process, or, even more ambitiously, to repair infarcted tissue. Improved infarct healing would mitigate the impact of MI on LV structure and function, and repair would potentially restore structure and function to previously damaged regions. Examples of the new therapeutic approaches include pharmacological, stem cell, and gene therapies, as well as tissue engineering and others [2].

MI occurs through the processes of cellular necrosis and apoptosis initiated by ischemia (and reperfusion). The natural infarct healing process begins shortly after MI with the release

of chemokines and cytokines that attract circulating leukocytes, specifically neutrophils and monocytes, to the infarcted region [3]. Monocytes differentiate into macrophages in the infarcted tissue [4]. Over the course of days to weeks, neutrophils and macrophages serve to clear away dead cells and other necrotic debris. In addition, macrophages release factors that contribute to the formation of granulation tissue as well as initiate endothelial cell proliferation and angiogenesis, providing the blood flow needed to support the process of wound healing [4]. Next, fibroblasts proliferate and generate extracellular matrix proteins including collagen that mechanically strengthen the infarcted region. Over time, the vascular network diminishes, fibroblasts undergo apoptosis, and the initial region of injury is replaced with a thin, but dense, collagenous scar [5]. Also, during the period of infarct healing and wall thinning, the LV dilates and adverse remodeling occurs [6, 7]. Given this complex and multifaceted infarct healing process, it is widely hypothesized that opportunities exist for new therapies that will lead to a smaller and stronger scar, and, ultimately, a reduction in wall stress and overall remodeling. It is further hypothesized that tissue repair and regeneration methods could eventually replace scar tissue with functional myocardium [2].

Imaging plays a central role in the evaluation of MI both clinically and in the assessment of new therapies. Traditionally, imaging has assessed LV structure, function, perfusion, and viability. The most common modalities used for cardiac imaging have been single photon emission computed tomography (SPECT) and echocardiography, with CT, positron emission tomography (PET), and magnetic resonance imaging (MRI) seeing increased use over the past decade. While conventional imaging to assess the structure, function, perfusion, and viability of the heart remains critically important, new imaging methods are being developed to assess the molecular and cellular events that underlie MI, infarct healing, and tissue repair, such as imaging apoptosis, inflammatory cell infiltration, molecular markers of angiogenesis, and the extracellular matrix proteins. These molecular and cellular imaging methods can reveal previously unavailable information about the biology of infarct healing and, when combined with conventional imaging, will elucidate the relationships between the molecular and cellular biology of infarct healing and higher level measurements of LV structure and function. In this article, we focus on recent advances in cellular and molecular imaging in MI and infarct healing, including SPECT, PET, and MRI of apoptosis, macrophages, angiogenesis, and the extracellular matrix.

Imaging Apoptosis in MI

The death of cardiomyocytes following ischemia-reperfusion occurs by two main and distinct mechanisms: apoptosis and necrosis. Apoptosis is programmed cell death characterized by cell shrinkage, condensation of chromatin, break-up of the nuclear envelope, budding of the cell membrane, and segregation of the cell into several apoptotic bodies. Apoptotic cells express anionic phospholipids like phosphatidylserine (PtdS) on the external surface of the cell membrane, which is recognized and phagocytosed by macrophages [8]. Because apoptosis is a sequence of specific intracellular events, it can be manipulated by various therapies and reversed. Necrosis on the other hand is the end stage of cell death and is irreversible. Apoptotic cells may have the potential to be salvaged if detected early.

Imaging of cell death provides valuable insights into the mechanisms and extent of myocardial cell loss, and may be useful in the development and evaluation of cardioprotective therapies. Several molecular targets have been used to detect apoptosis in MI or ischemia-reperfusion, the most common being Annexin-V (Anx), which binds to externalized PtdS on apoptotic cells. For example, Anx has been conjugated with several contrast agents like Technetium-99 (^{99}Tc) for SPECT imaging [9–11], probes for fluorescence imaging [12], and magneto-optical nanoparticles for MRI [13]. Examples using other targets include the work of Fang et al. [14], which used the ^{99m}Tc-labeled C2A domain of synaptotagmin I with SPECT imaging in a porcine ischemia-reperfusion model, and the work of Zhao et al. [15] that evaluated ^{99m}Tc-labeled duramycin as a novel molecular probe for imaging phosphatidylethanolamine, which is found in apoptotic and necrotic cells.

Recently there has been a growing interest in differentiating between apoptosis and necrosis *in vivo* using a dual-contrast approach, as this would identify apoptotic but viable myocardium which could potentially be salvaged. In 2008, Sarda-Mantel et al. [16•] used a dual-contrast technique to illustrate the spatio-temporal course of apoptosis and necrosis using SPECT imaging. ^{99m}Tc–annexin-V was used to target apoptosis and ^{111}In-antimyosin antibodies (AM) were used to detect necrosis, as it is specific for myosin on ruptured cell membranes. A rat 20-min occlusion-reperfusion model was used. Rats were injected with Anx, AM, or both and the uptake of the two tracers was evaluated using SPECT, autoradiography, and histology at 2, 4, and 24 h post-MI. They showed that apoptosis illustrated by Anx uptake started as early as 2 h post-MI and was primarily in the mid-myocardium. However, necrosis shown by AM uptake using autoradiography started 3 h post-MI and occurred mostly in the endocardial and epicardial myocardium. Anx and AM uptake decreased by 24 h post-MI, suggesting that most of the dead cells are removed from the mid-myocardium by 24 h post-MI.

Using another dual-contrast approach, Sosnovik et al. [17•] recently demonstrated combined imaging of cardiomyocyte (CM) apoptosis and necrosis *in vivo* using

molecular MRI. This study used the annexin-based iron-oxide nanoparticle AnxCLIO-Cy5.5 to target apoptosis and a novel gadolinium chelate Gd-DTPA-NBD to detect necrosis. The gadolinium chelate allowed the visualization of necrosis via delayed enhancement (DE) imaging and the conjugation of 7-nitrobenz-2-oxa-1,3-diazol-4-yl (NBD) allowed the detection of necrosis by histology. Mice were subjected to 35 min of coronary occlusion followed by reperfusion, after which they were injected with either AnxCLIO-Cy5.5 or control InactCLIO-Cy5.5. T_2^*-weighted MR images were acquired 4 to 6 h post-reperfusion (Fig. 1). The contrast-to-noise ratio (CNR) of injured to normal myocardium in the AnxCLIO-Cy5.5 group was significantly greater as compared to the control group, demonstrating the specificity of the tracer for apoptotic cells. AnxCLIO-Cy5.5 was mostly concentrated in the mid-myocardium. Following this, Gd-DTPA-NBD was injected and MRI showed the presence of necrosis in only about 21% of the myocardial region with AnxCLIO-Cy5.5. This suggested that greater than 70% of injured myocardium showed exclusive accumulation of AnxCLIO-Cy5.5 and is viable and potentially salvageable. These results were confirmed by fluorescence microscopy of AnxCLIO-Cy5.5 and immunohistochemistry of Gd-DTPA-NBD.

Imaging Inflammation in Infarct Healing

During the infarct healing process macrophages infiltrate the infarct zone within a few days of the ischemic event and play a number of key roles, including secreting cytokines and growth factors, clearing necrotic debris, promoting angiogenesis, and influencing extracellular matrix composition. Given their prominent roles in infarct healing and their potential as therapeutic targets, cellular imaging of infiltrating macrophages has been of increasing interest in recent years, mainly using MRI. For example, in 2007, Sosnovik et al. [18] demonstrated that intravenous injection of magneto-fluorescent iron-oxide nanoparticles 2 days after experimental MI could be used to label macrophages, and that the labeled cells could be detected 2 days later in the infarcted region of the heart using T_2*-weighted MRI. Using a related but different approach, in 2008 Flogel et al. [19] performed *in vivo* labeling of macrophages with an intravenous injection of a nanoemulsion of perfluorocarbons (PFCs) and used lower-resolution ^{19}F MRI to detect the signal 1 to 6 days later. To determine the position of the labeled macrophages relative to other anatomy (which does not have any ^{19}F signal), the ^{19}F signal was overlaid in color on a conventional high-resolution ^{1}H MR image of the heart. These methods showed that macrophages were spatially confined to the region of infarction, and also that, temporally, macrophages could be detected in the heart for at least 6 days after MI. In addition to imaging endogenous macrophages, Leor et al. [20] demonstrated MRI tracking of iron-labeled macrophage cell therapy. In this study, therapeutic human activated macrophage suspension (AMS) was labeled with iron oxide nanoparticles *ex vivo*, and then injected into the infarct zone in a rat model of MI. Serial T_2*-weighted MRI noninvasively verified the presence of labeled cells throughout the study, which showed that AMS accelerates angiogenesis and infarct repair, and reduced post-MI LV remodeling.

In the papers by Sosnovik et al. [18] and Flogel et al. [19], inflammatory cells were labeled by intravenous injection after MI. A limitation of labeling inflammatory cells after MI is that resident inflammatory cells in the infarct zone can endocytose contrast agent that extravasates from plasma. Thus, this method cannot distinguish between infiltration of labeled inflammatory cells originating outside the infarcted tissue and inflammatory cells that are already present in the lesion which phagocytose extravasated

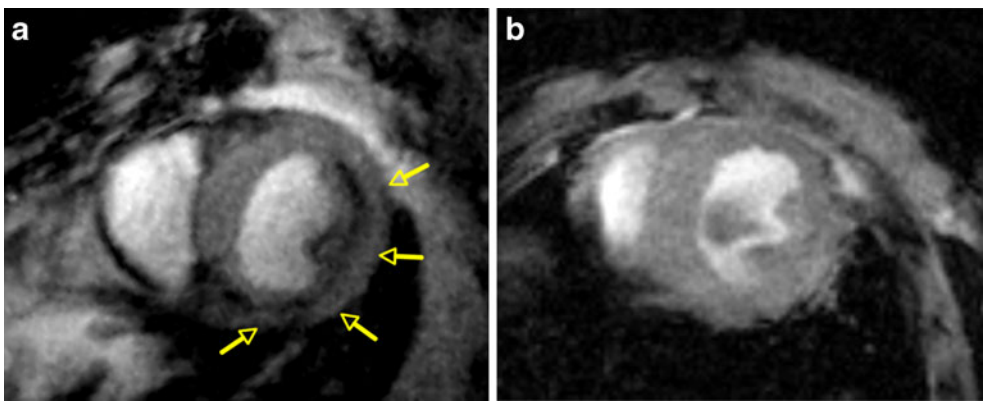

Fig. 1 Molecular MRI (echo time, 4 ms) of cardiomyocyte apoptosis in myocardium exposed to mild-moderate injury. **a**, Mouse injected with AnxCLIO-Cy5.5. **b**, Mouse with a similar degree of injury but injected with the control (annexin-inactivated) agent Inact_CLIOCy5.5. Significant mid-myocardial uptake of the active probe (signal hypointensity) is seen in the region of injury (*yellow arrows*). No significant uptake of the control probe is seen (**b**). (*Reprinted with permission from* Sosnovik et al. [17•])

contrast agent. Recently two studies by Montet-Abou et al. [21•] and Yang et al. [22] investigated labeling inflammatory cells with iron oxide particles prior to MI, and then using MRI to monitor the infiltration of these cells into the site of the MI.

In the study by Montet-Abou et al. [21•], rats were injected with fluorescent iron-oxide particles 3 days prior to MI, allowing time for the particles to clear from the plasma before inducing MI. The animals were divided into four categories: 1) SPION_MI (superparamagnetic iron oxide nanoparticles [SPION] labeled rats with MI); 2) SPION_Sham (labeled rats with sham operation); 3) φ_MI (non-labeled rats with MI); and 4) SPION_MI_AntiCCL5 (SPION-labeled rats with MI and anti-inflammatory treatment where CCL5 is an inflammatory chemokine). Serial *in vivo* MRI was performed on days 0 to 3 post-MI and the results were confirmed by serial *ex vivo* imaging (MRI and reflectance fluorescence) and histology. A consistent hypointense signal verifying the presence of iron-oxide particles was found in the infarct region in the SPION_MI group using T_2*-weighted MRI while no hypointense signal was found in the φ_MI and SPION_Sham groups (Fig. 2). A smaller hypointense region was found in the SPION_MI_AntiCCL5 group using *in vivo* and *ex vivo* imaging. Histology indicated the presence of numerous CD68-positive cells (monocytes/macrophages) containing iron in the SPION_MI group, while no iron was detected in the φ_MI group and no CD68-positive cells were found in the SPION_Sham group. The SPION_MI_AntiCCL5 group showed very few CD68-positive cells containing iron. These results substantiated the infiltration of monocytes/macrophages preloaded with fluorescent iron-oxide particles into the MI region. In addition to observing MRI signal loss due to labeled cells, multi-echo data were also acquired and T_2 values were quantified. The $1/T_2$ value was highest in SPION_MI, intermediate in SPION_MI_An-

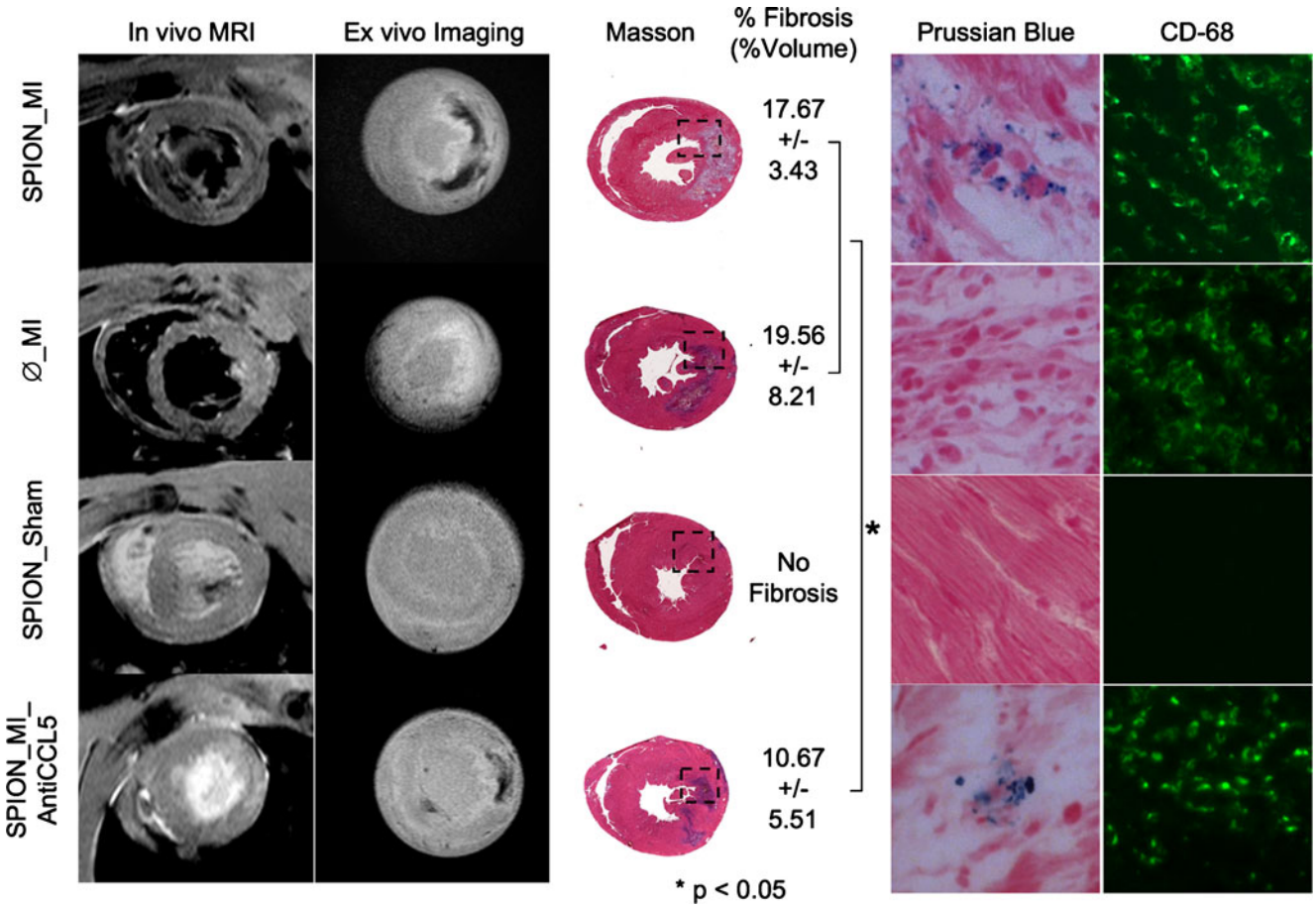

Fig. 2 *In vivo* and *ex vivo* imaging of monocytes at day 3 post–myocardial infarction (MI) labeled using iron oxide nanoparticles 3 days before MI and its comparison with all groups at day 3. SPION_MI clearly showed a hypointense signal by MRI (*in vivo* and *ex vivo*) in the MI. The fibrosis of this group was calculated to 17.67% +3.43% (%vol). There were numerous fluorescent-loaded cells in the MI, corresponding to CD68-positive cells. Ø_MI did not show hypointense signal by MRI, or iron-loaded cells by histology. The fibrosis was 19.56%+8.21%. The SPION_Sham group did not show an inflammatory infiltrate or MI. The SPION_MI_AntiCCL5 showed a hypointense signal by MRI, smaller fibrosis (10.67%+5.51%), and less iron-loaded CD68-positive cells in the MI. * $P<0.05$. (*Reprinted with permission from* Montet-Abou et al. [21•])

tiCCL5, and lowest in φ_MI group. Thus, using *in vivo* and *ex vivo* imaging, Montet-Abou et al. showed that monocytes/macrophages can be preloaded with fluorescent iron-oxide nanoparticles and then their infiltration into infarcted myocardium can be tracked over the course of multiple days.

In another recent MRI study, Yang et al. [22] used a pre-MI injection of micrometer-sized iron oxide (MPIO) particles to label inflammatory cells, and observed the mouse heart over a longer time period. Specifically, cells were labeled 7 days pre-MI and CNR at the MI site was used to measure cell infiltration for 14 days after MI. The results showed consistent infiltration of MPIO-labeled inflammatory cells (mostly macrophages) into the MI region beginning at day 3 post-MI and persisting to day 14. While the detection of labeled cells in the infarct zone between days 3 and 7 post-MI is expected, since prior non-imaging histological studies have shown that macrophage density decreases progressively after day 4 post-MI in mice [23, 24], the apparent consistent presence of labeled macrophages at day 14 may call into question the results obtained using MPIO-labeled cells at later time points.

Even more recently Naresh et al. [25] investigated pre-labeling monocytes using a T_1-shortening, rather than T_2-shortening, contrast agent. Specifically, liposomes incorporating gadolinium-DPTA-bis(stearylamide) (Gd-liposomes) were injected intravenously (50–100 μL) in five mice 2 days before MI to label inflammatory cells. MI was induced at day 0 by a 1-hour occlusion of the left anterior descending coronary artery followed by reperfusion. MRI T_1-mapping of the heart was performed at days −3 and −1 before MI, and days 1, 4, and 7 post-MI. The T_1 of the infarcted anterolateral wall was normal at days −3, −1, and 1, was significantly decreased at day 4, and returned to normal at day 7. Spatially, T_1 shortening was confined to the dysfunctional infarct zone at all time points. T_1 mapping of the spleen showed that monocytes remain labeled with Gd-liposomes through day 7 post-MI. This study concluded that T_1-mapping after pre-labeling monocytes with Gd-liposomes enabled the quantitative measurement of macrophage infiltration of the infarct zone after MI. The spatiotemporal macrophage kinetics measured *in vivo* using these techniques, including washout by day 7, agreed with prior *in vitro* histological studies [23, 24]. Figure 3 demonstrates T_1-weighted MRI of macrophages labeled using Gd-liposomes, where the specific methods have been described previously [26].

While the previously described techniques treated all monocytes/macrophages as a homogeneous cell type, recent work has shown that there are in fact two subsets of this cell type, Ly-6C^{high} and Ly-6C^{low} macrophages. The Ly-6C^{high} macrophages are activated and participate in digesting damaged tissue and clearing necrotic debris, while the Ly-6C^{low} macrophages promote wound healing, angiogenesis, and scar formation [27]. Furthermore, it is thought that it may be possible to manipulate the ratio of Ly-6C^{high}/Ly-6C^{low} macrophages to improve infarct healing. In this context, Panizzi et al. [28•] showed that fluorescence molecular tomography (FMT) targeting cathepsin selectively images Ly-6C^{high} macrophages, and demonstrated that an increase in the number of Ly-6C^{high} macrophages perturbs infarct healing and contributes to greater LV remodeling.

In related work, Nahrendorf et al. [29•] recently investigated MRI of myeloperoxidase (MPO) activity in MI. MPO is an enzyme most likely introduced by activated inflammatory cells like neutrophils and monocytes in ischemic myocardium [27]. MPO induces production of cytotoxic oxidants that are detrimental to post-MI LV remodeling and cardiac function [30, 31]. Nahrendorf et al. [29•] introduced a Gd-based sensor activated by MPO (MPO-Gd) that polymerizes and causes signal amplification and enhanced retention in regions with high MPO activity. They illustrated the specificity and sensitivity of this agent to MPO, and used it to image MPO noninvasively after MI, where it was found to be colocalized with neutrophils and monocytes. Furthermore, using serial MPO imaging post-MI, they demonstrated

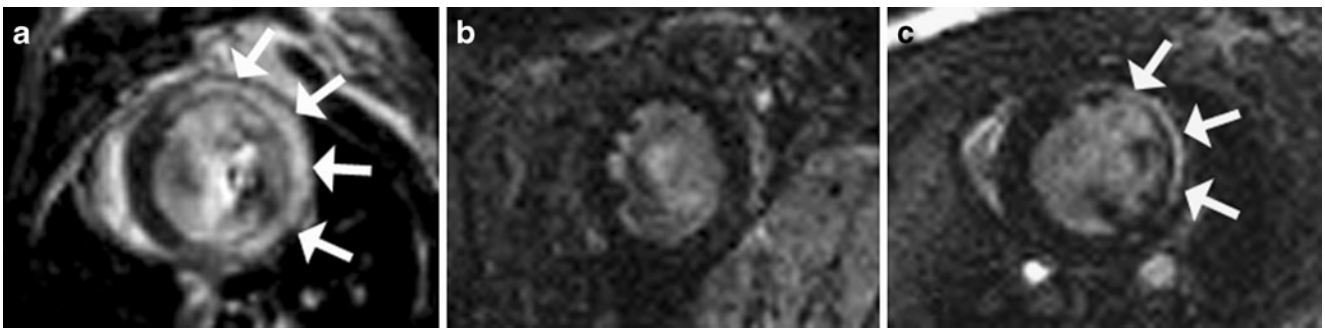

Fig. 3 Tracking post–myocardial infarction (MI) macrophage infiltration using Gd-liposomes. Gd-DTPA–enhanced inversion-recovery (IR) MRI demonstrates the region of infarction 2 days after MI (**a**, *arrows*). No myocardial enhancement was seen at day 2 post-MI before administering Gd-DTPA and after administering Gd-liposomes (**b**). However, on day 4 post-MI (**c**), macrophages labeled with Gd-liposomes have infiltrated the infarct zone and show enhancement on IR images (*arrows*)

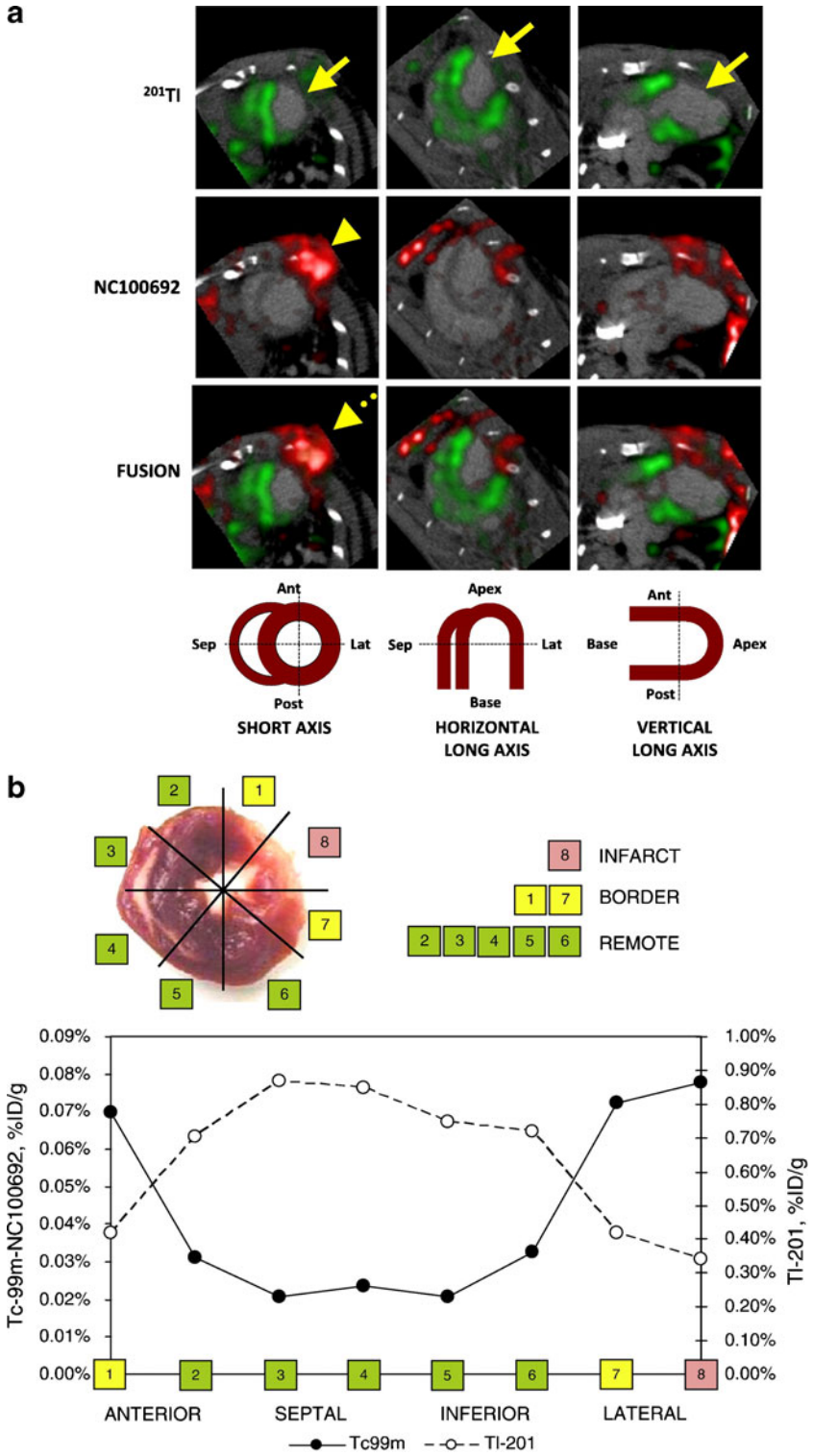

Fig. 4 SPECT imaging of α_v integrins. **a**, In vivo microSPECT-CT images of ^{201}Tl perfusion (*top row, green*) and ^{99m}Tc-NC100692 (*middle row, red*) in IGF-1 rat at 4 weeks post–myocardial infarction (MI) were reconstructed in short and horizontal and vertical long axes and fused (*bottom row*) with a reference contrast CT image (grayscale). All post-MI rats had an anterolateral ^{201}Tl perfusion defect (*yellow solid arrows*) and focal uptake of ^{99m}Tc-NC100692 in defect area. The contrast agent permitted better definition of myocardium allowing differentiation of focal myocardial uptake of targeted radiotracer from uptake within chest wall at the thoracotomy site (*dashed yellow arrows*). **b**, Representative circumferential count profile of middle myocardial section of IGF-1 rat at 4 weeks post-MI. Count profiles for both ^{99m}Tc-NC100692 (*solid circles*) and ^{201}Tl perfusion (*open circles*) are demonstrated. (*Reprinted from* Dobrucki et a1. [36•], with permission from Elsevier)

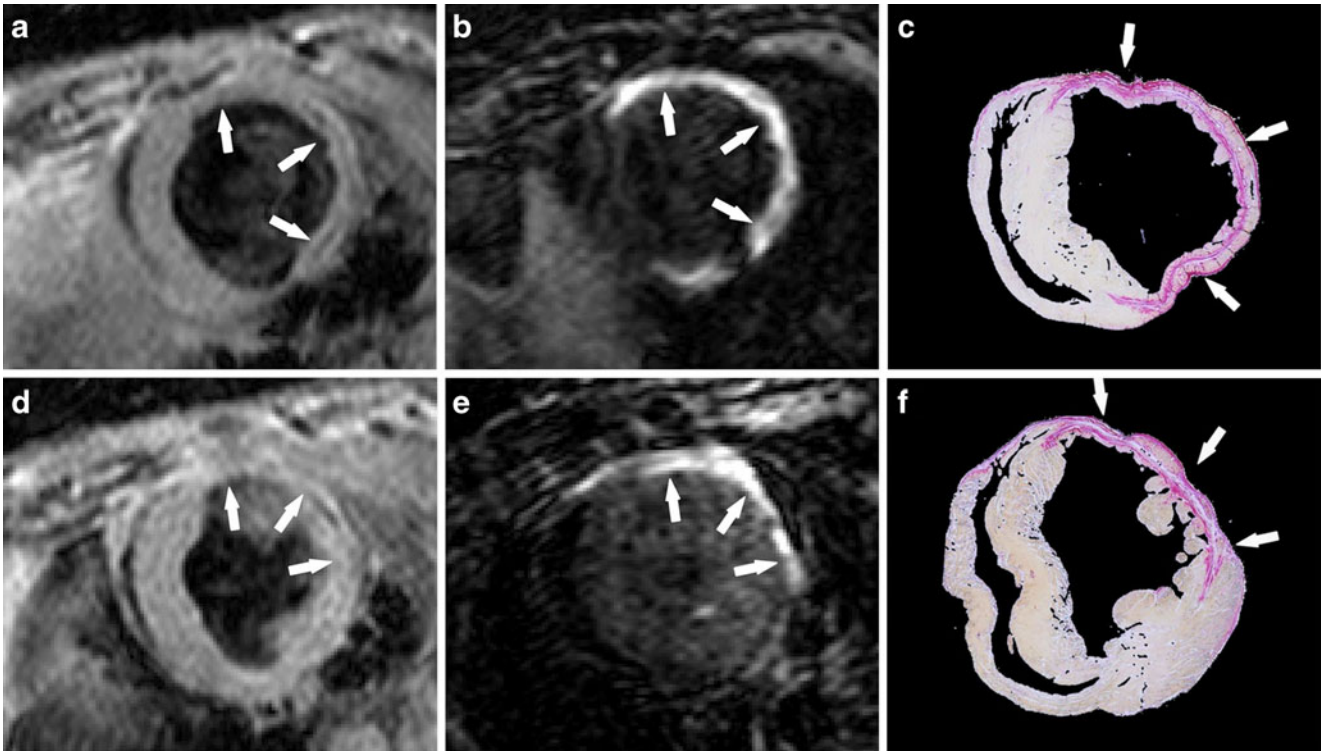

Fig. 5 Imaging of fibrosis and scar post–myocardial infarction using a collagen-targeted contrast agent. Gradient-echo inversion-recovery (IR) MRI (**b**, **e**) and corresponding picrosirius red–stained histologic sections of the left ventricle (**c**, **f**). *Arrows* point to area of scarring. Standard anatomic MRIs acquired by using a double IR gradient-echo sequence (**a**, **d**). Regions of contrast enhancement on midventricular short-axis MRIs of the left ventricle at two section locations obtained 40 min after EP-3533 injection correlate closely with photomicrographs of picrosirius red–stained tissue sections shown at nine times their original size. (*Reprinted with permission from* Helm et al. [41•])

the temporal course of MPO with a peak at day 2 post-MI. They also successfully detected the anti-inflammatory effects of atorvastatin using these methods.

Imaging Angiogenesis in Infarct Healing

Angiogenesis is defined as the growth and formation of new blood vessels from pre-existing vasculature. It occurs naturally after MI and supplies the healing infarct with the blood flow, oxygen, and nutrients needed to support processes from clearing necrotic debris to forming the collagen scar. In addition, therapies to enhance angiogenesis have shown potential for reducing post-MI LV remodeling, and for supporting reparative and regenerative therapies such as stem cells. Molecular imaging of angiogenesis has been investigated in a number of settings, including in cancer, atherosclerosis, and healing MI. In infarct healing, both the $\alpha_v\beta_3$ integrin, a cell surface integrin expressed on proliferating endothelial cells, and the vascular endothelial growth factor (VEGF) receptor have been used as markers of angiogenesis. In addition, both SPECT and PET modalities have been investigated for post-MI angiogenesis imaging, using a number of different targeting ligands. For example, Meoli et al. [32] first demonstrated the feasibility of imaging post-MI angiogenesis using SPECT with the radiotracer ^{111}In-RP748, a quinolone targeting the $\alpha_v\beta_3$ integrin. This method was applied in both rats and dogs, where signal from ^{111}In-RP748 was clearly localized to the region of infarction in both *in vivo* images and, at higher spatial resolution, in *ex vivo* images of tissue slices. Also targeting the $\alpha_v\beta_3$ integrin, Higuchi et al. [33•] used PET with ^{18}F-Galacto-RGD to monitor the time course of post-MI angiogenesis in rats, showing an initial increase in uptake ratio 3 days post-MI, with a peak at 1 to 3 weeks post-MI, and then a decreasing uptake ratio 3 to 6 months post-MI. In contrast to imaging $\alpha_v\beta_3$ integrin expression, Rodriguez-Porcel et al. [34•] used PET with ^{64}Cu-DOTA-VEGF$_{121}$ to image upregulation of the VEGF receptor as a marker of post-MI angiogenesis in a rat model of permanent coronary occlusion. In this study, PET imaging localized post-MI VEGF receptor upregulation to the infarct zone, and showed greatest intensity 3 days post-MI followed by sequentially diminishing intensity on days 10 to 24 post-MI. Different ischemia protocols and/or different molecular targets may explain the different time courses observed in these studies.

Recently, Dimastromatteo et al. [35] evaluated another novel SPECT agent and showed that ^{99m}Tc-RAFT-RGD is

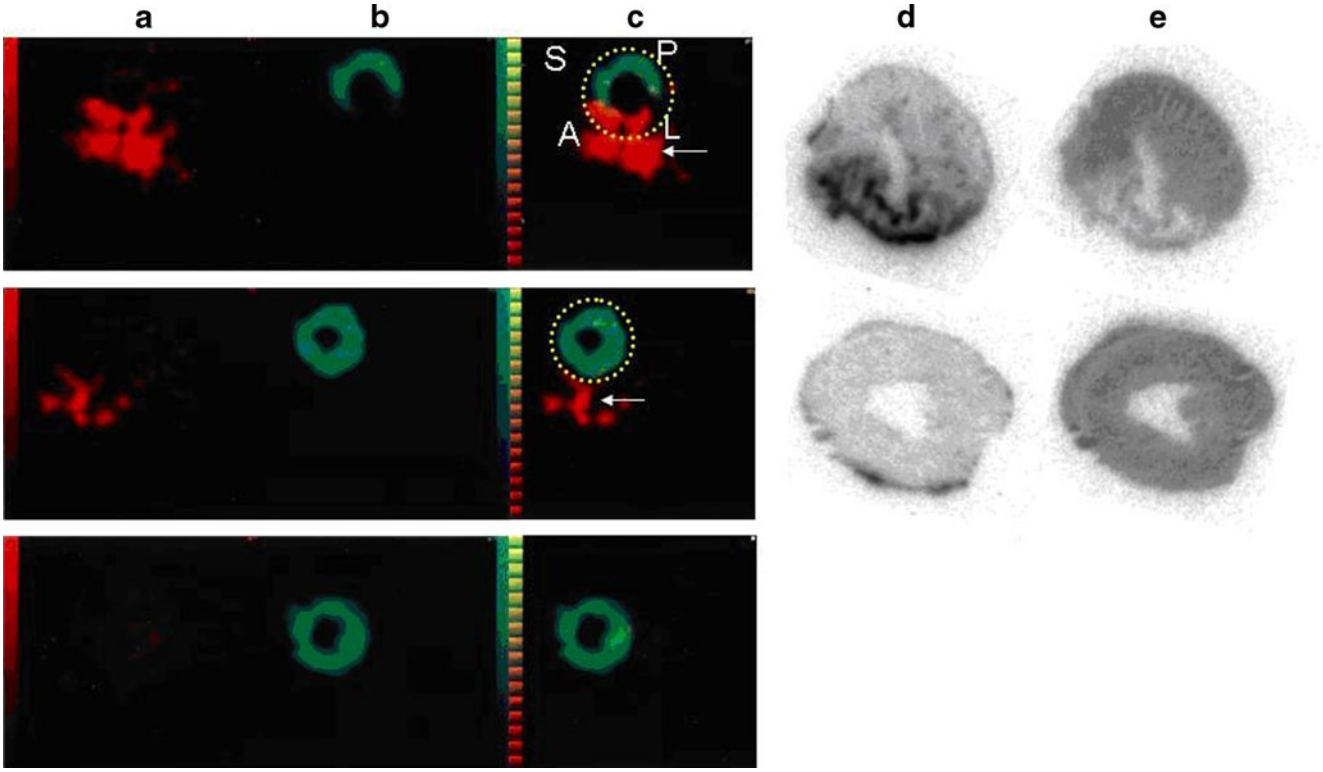

Fig. 6 In vivo SPECT imaging of tenascin-C. Comparison of SPECT imaging between ^{111}In-anti-TNC-Fab and ^{99m}Tc MIBI. Transverse dual-isotope SPECT images (**a**–**c**) and autoradiographies of the same rats (**d**, **e**). The uptake of ^{111}In-anti-TNC-Fab (*red* in **a**, **c**, **d**) and ^{99m}Tc-MIBI (*green* in **b**, **c**, **e**) in acute myocardial infarction heart (*upper panels*), in sham-operated heart (*middle panels*), and in normal rat heart (*lower panels*). *Red color* indicates the uptake of ^{111}In-anti-TNC-Fab and *green color*, the uptake of ^{99m}Tc-MIBI. *Yellow broken lines* circle myocardium. *White arrows* indicate sutured incision of the left intercostal space just below the myocardium. A, anterior left ventricular wall; L, lateral left ventricular wall; P, posterior left ventricular wall; S, septal wall. (*Reprinted with permission from* Odaka et al. [44•])

also well-suited for *in vivo* molecular imaging of post-MI angiogenesis. Regioselectivity Addressable Functionalised Template-RGD (RAFT-RGD) is composed of four cyclo (RGDfK) sequences attached to a peptide that binds to the $\alpha_v\beta_3$ integrin. The RGD molecules are co-internalized with the receptor, which may increase the affinity of the peptide for the $\alpha_v\beta_3$ integrin. A rat model of reperfused MI was employed for this study, where 14 days after MI rats were injected with either ^{99m}Tc-RAFT-RGD or its negative control ^{99m}Tc-RAFT-RAD. Rats underwent *in vivo* dual-isotope SPECT imaging of ^{201}TI and ^{99m}Tc-RAFT-RGD or ^{99m}Tc-RAFT-RAD. The infarct-to-normal zone activity ratio was significantly higher with ^{99m}Tc-RAFT-RGD compared to ^{99m}Tc-RAFT-RAD. Also consistent ^{99m}Tc-RAFT-RGD uptake was observed throughout the infarct zone as delineated by the ^{201}TI perfusion defect. For control studies using ^{99m}Tc-RAFT-RAD, there was no preferential uptake in the infarct zone. In comparing this contrast agent to those evaluated in prior studies, the infarct-to-normal zone activity ratio was 2.5 for SPECT with ^{99m}Tc-RAFT-RGD, which is somewhat higher than the values obtained by Meoli et al. [32] using SPECT with ^{111}In-RP748 and is comparable to the value achieved by Higuchi et al. [33•] using PET with ^{18}F-Galacto-RGD.

Building on the pioneering studies that developed various methodologies for nuclear imaging of post-MI angiogenesis, Dobrucki et al. [36•] recently applied targeted SPECT imaging of α_v integrins and conventional echocardiography of LV structure and function to investigate the role of insulin-like growth factor-1 (IGF-1) in infarct healing and LV remodeling. In this study, after induction of MI, the human IGF-1 gene was delivered by injection of an adeno-associated virus (AAV-IFG-1) to the peri-infarct zone of infarcted rat hearts. Control rats were injected with AAV-lacZ. SPECT imaging was performed at 4 and 16 weeks post-MI using ^{99m}Tc-labeled RGD peptide (NC100692, GE Healthcare) to assess angiogenesis, and using ^{201}TI chloride to assess perfusion. Immunohistochemistry showed a marked increase in capillary density in AAV-IFG-1 hearts compared to controls, and SPECT revealed significantly higher α_v integrin activation in the hypoperfused infarcted regions of the IGF-1 group relative to controls at 4 weeks post-MI (Fig. 4), although the activation was reduced at 16 weeks post-MI. Transthoracic

Table 1 Imaging of the different phases of infarct healing

Phase	Imaging modality	Label/probe	Target	Studies
Cell death (apoptosis and necrosis) Fig. 7a	SPECT	^{99m}Tc-labeled C2A domain of synaptotagmin I	Apoptosis	[14]
		^{99m}Tc-labeled duramycin	Apoptosis, necrosis	[15]
		^{99m}Tc-annexin-V	Apoptosis	[16•]
		^{111}In-antimyosin antibodies	Necrosis	[16•]
	MRI	AnxCLIO-Cy5.5	Apoptosis	[17•]
		Gd-DTPA-NBD	Necrosis	[17•]
Cell infiltration into the infarct, inflammation Fig. 7b	MRI	Iron-oxide nanoparticles	Macrophages	[18, 20, 21•]
		Micro-meter iron oxide particles	Inflammatory cells (mostly macrophages)	[22]
		Nanoemulsion of perfluorocarbons	Macrophages	[19]
		Gd-liposomes	Monocytes	[25]
		MPO-Gd	Myeloperoxidase	[29•]
	FMT	Cathepsin	Ly-6C^{high} macrophages	[28•]
Angiogenesis, ECM deposition Fig. 7c	SPECT, SPECT-CT	Radiotracer ^{111} In-RP748	$\alpha_v\beta_3$ integrin	[32]
		^{99m}Tc-RAFT-RGD	$\alpha_v\beta_3$ integrin	[35]
		^{99m}Tc-labeled RGD	$\alpha_v\beta_3$ integrin	[36•]
		^{201}TI chloride	To assess perfusion	[36•]
	PET	^{18}F-Galacto-RGD	$\alpha_v\beta_3$ integrin	[33•]
		^{64}Cu-DOTA-VEGF	$VEGF_{121}$	[34•]
	MRI	cNRG-pQDs	CD13	[37]
Left ventricular remodeling and scar formation Fig. 7d	Echocardiography			[36•]
	SPECT-CT	^{99m}Tc-RP805	MMPs	[39]
		^{111}In-DOTA-FXIII	FXIII	[48•]
	MRI	EP-3533	Collagen	[41•]
	SPECT	^{111}In-anti-TNC-FAB	Tenascin-C	[44•]
		^{125}I-TNC-Ab	Tenascin-C	[45]
		^{99m}Tc-CRIP	$\alpha_v\beta_3$ integrin	[46]
		^{99m}Tc-streptavidin-collagelin	Collagen	[43]

echocardiography at 16 weeks showed less LV remodeling and enhanced cardiac function in the IGF-1 group as compared to the control group. These results, which were largely based on molecular imaging of angiogenesis by SPECT, perfusion imaging by SPECT, and imaging of LV function by echocardiography, demonstrated a potential therapeutic role for IGF-1 in enhancing myocardial angiogenesis in the early phase of infarct healing and reducing long-term post-MI LV remodeling.

In addition to nuclear methods, Oostendorp et al. [37] recently investigated using MRI with cyclic Asn-Gly-Arg (cNGR)–labeled paramagnetic quantum dots (pQDs) for imaging post-MI angiogenesis. The contrast agent cNGR-pQDs, synthesized by conjugating Gd-labeled pQDs with cNGR tripeptide, targets CD13, a membrane-bound aminopeptidase that is exclusively expressed on endothelial cells of angiogenic vessels in ischemic myocardium. In this study, mice were divided into three groups: MI + cNGR-pQDs, MI + unlabeled-pQDs, and sham + cNGR-pQDs. Seven days following infarct surgery, contrast agent was injected and gradient echo images were acquired from 30 min–2 h post contrast injection. Negative contrast in the infarct and border regions was measured in the MI + cNGR-pQDs group, which was significantly different than the control groups. *Ex vivo* three-dimensional 2-photon laser scanning microscopy showed that the cNGR-pQDs were colocalized with vascular endothelial cells in the infarct/border zone. Thus, this study demonstrated that MRI with cNGR-pQDs can detect post-MI myocardial angiogenesis. However, a potential limitation is that the method may not be quantitative, and therefore may not be well-suited for serial studies that aim to quantify the degree of angiogenesis as it changes over time. Nonetheless, this study does demonstrate the feasibility of imaging post-MI angiogenesis with MRI, suggesting that post-MI angiogenesis MRI may be further improved in the future and then combined with other MRI measurements of structure, perfusion, and function, to potentially provide a highly comprehensive imaging examination.

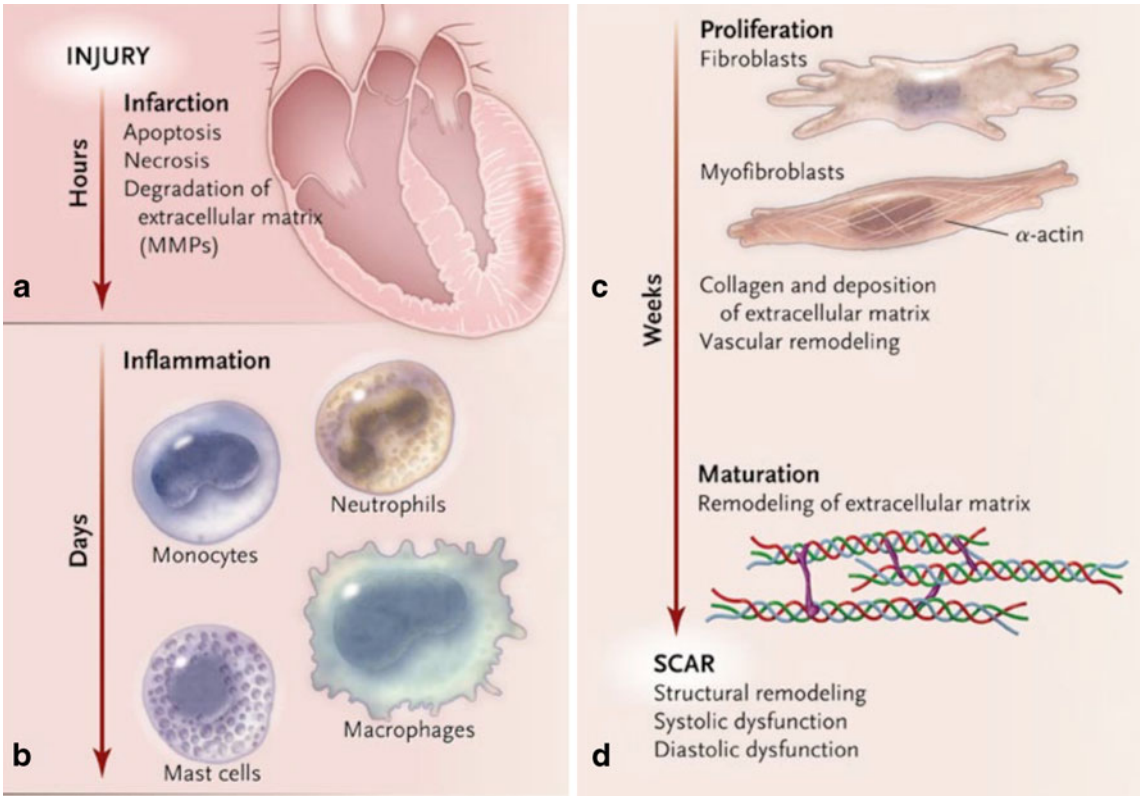

Fig. 7 Different phases of infarct healing. (*Reprinted with permission from* Jugdutt [49])

Imaging the Extracellular Matrix in Infarct Healing

The extracellular matrix (ECM) is foundational to cardiac (and other) tissue, providing structural support for tissue and cells, anchoring cells, and participating in cell signaling. In acute MI and infarct healing, the ECM plays a central and increasingly appreciated role [38]. Early after MI, the ECM is rapidly degraded by proteases secreted from inflammatory cells, and in subsequent stages of infarct healing fibroblasts regenerate the ECM, helping to form granulation tissue, promoting angiogenesis, and eventually forming the dense collagen scar. Given the important roles of the ECM in post-MI structural remodeling, molecular imaging of ECM physiology during infarct healing is receiving growing attention. In 2005, two studies investigated molecular imaging of matrix metalloproteinases (MMPs), which are secreted by inflammatory cells, degrade the ECM, and have been shown to have a significant impact on post-MI LV remodeling in animal models. Specifically, Su et al. [39] developed a ^{99m}Tc-labeled MMP-targeted radiotracer (^{99m}Tc-RP805) and used it with SPECT-CT to detect MMPs 1 to 3 weeks post-MI. In another study by Chen et al. [40], *ex vivo* near-infrared fluorescent imaging with a probe activated by proteolytic cleavage by MMP-2 and MMP-9 was developed and used to investigate the time course of MMP activity during infarct healing.

More recently, Helm et al. [41•] employed a gadolinium-based collagen-targeting contrast agent (EP-3533) to perform molecular MRI of scar in a mouse model of healed MI. Post-MI scar ECM contains a high concentration of type I collagen, making it a suitable target for molecular MRI based on a T_1 shortening contrast agent. EP-3533 was designed by appending gadopentetate dimeglumine moieties to a collagen-specific peptide. The structure, full synthesis, and synthetic characterization of EP-3533 have been described previously in detail [42]. Mice were imaged using MRI 6 weeks after experimental MI created by a 60-minute coronary artery occlusion followed by reperfusion. Dynamic T_1-weighted MRI acquired over 50 min after contrast agent injection showed a substantially longer washout time constant for EP-3533 (195 min) than for conventional gadopentetate dimeglumine (25 min) in regions of scar. Also, postmortem histological sections stained with picrosirius red for collagen correlated well with EP-3533–enhanced areas seen on matched T_1-weighted MRI slices (Fig. 5). Lastly, inductively coupled plasma mass spectrometry showed that 50 min after EP-3533 injection, scar tissue samples had a two-fold higher concentration of gadolinium compared to normal myocardium. This study concluded that EP-3533 enables *in vivo* positive-contrast molecular MRI of fibrosis and scar in a mouse model of healed MI. In a related study, Muzard et al. [43] developed a collagen-specific probe

Table 2 Advantages and disadvantages of imaging modalities for infarct healing

Imaging modality	Advantages	Disadvantages
SPECT	• High sensitivity	• Radiation
	• Broad range of radioisotope half-lives compared to PET	• Relatively low spatial resolution
	• Multi-spectral	• Photon attenuation correction more challenging compared to PET
	• Relatively low cost	
	• Widely available	• Longer scan time compared to PET
PET	• Very high sensitivity	• Radiation
	• Attenuation correction easier than SPECT	• Radioisotopes have shorter half-lives than SPECT
	• Radiotracers more similar to naturally occurring biological compounds compared to SPECT	• High cost compared to SPECT
MRI	• High spatial resolution	• Lower sensitivity to molecular-imaging tracers
	• Good soft-tissue contrast	
	• Good for functional and anatomical imaging	• Problematic for patients with devices
	• No radiation	
	• Suitable for serial studies	
Echocardiography	• Low cost	• Subjective examination depending on operator skill
	• No radiation	
	• Widely available	• Molecular imaging is limited to intravascular targets
	• Short scan time	
	• Convenient examination	• Image quality depends on availability of adequate acoustic window
	• Good structure information	
FMT	• No radiation	• Not applicable to human heart due to poor penetration
	• Quantitative	• Background autofluorescence

called Collagelin to target post-MI fibrosis using SPECT in a rat model.

Other recent work has investigated targeted imaging of tenascin-C [44•, 45], an extracellular matrix glycoprotein that appears transiently after MI and is thought to facilitate the recruitment of fibroblasts to the infarct zone by weakening the links between cardiomyocytes and the ECM. For this, Odaka et al. [44•] used ^{111}In-labeled anti-tenascin-C-FAB, and rats were imaged both *in vivo* by SPECT (Fig. 6) or *ex vivo* using autoradiography. More recently, Taki et al. [45] used ^{125}I-labeled anti–tenascin-C antibody with autoradiography to demonstrate the spatio-temporal time course of post-MI tenascin-C expression in rats, showing initial expression at day 1 post-MI, a peak at day 3, and then a reduction 7 to 14 days post-MI. Spatially, autoradiography in one study [44•] found greater tenascin-C expression at the border of the infarct zone, but this was not replicated by Taki et al. [45]. For clinical translation, ^{111}In-anti-TNC-FAB or ^{123}I-TNC-Ab may be useful SPECT agents.

In addition to MMPs, collagen, and tenascin-C, van den Borne et al. [46] sought to image myofibroblast proliferation as an indicator of post-MI increases in collagen production and fibrosis. ^{99m}Technetium-labeled Cy5.5-RGD imaging peptide (CRIP) was used to target the $\alpha_v\beta_3$ integrin, which is on the cell membrane of myofibroblasts. SPECT was performed *in vivo* in mice 2, 4, and 12 weeks after MI, CRIP uptake was found to be greatest in the infarct zone at 2 weeks, and CRIP uptake underwent stepwise decreases at 4 and 12 weeks. Anti-angiotensin treatment with captopril and losartan decreased the degree of fibrosis and CRIP uptake. The authors concluded that SPECT with radiolabeled CRIP enables imaging of interstitial alterations during cardiac remodeling.

Blood coagulation factor XIII (FXIII) is a protransglutaminase that is important in strengthening the ECM during infarct healing [47]. In a study by Nahrendorf et al. [48•], the authors demonstrated the beneficial effects of FXIII on infarct healing and LV remodeling noninvasively using SPECT-CT in a mouse model of permanent coronary ligation. The mice were divided into three groups: control, FXIII-treated, and dalteparin (DP)-treated mice. DP is comparable to heparin, which is an anticoagulant. *In vivo* SPECT-CT imaging was performed using ^{111}In-DOTA-FXIII, which is identified by FXIII and bound to ECM proteins resulting in local entrapment of ^{111}In-DOTA-FXIII in the infarcted region. The imaging results revealed increased levels of FXIII within the infarct region in the FXIII group and diminished FXIII within the DP group, and these results were confirmed using autoradiography. Furthermore, using serial MRI, they showed reduced LV remodeling in the FXIII group while the DP group

exhibited increased mortality. Histological findings in the FXIII group revealed faster resolution of neutrophils, increased macrophages, improved angiogenesis (higher capillary density and VEGF), and collagen synthesis (increased myofibroblasts, collagen content). Thus, they exhibited the therapeutic potential of FXIII treatment in infarct healing in mice.

Conclusions

Significant progress has been made in recent years in molecular imaging of infarct healing and repair in animal models (Table 1; Fig. 7). For example, MRI can detect and monitor MPO activity, cellular processes such as macrophage infiltration, and microstructural changes such as collagen deposition. MRI and SPECT can identify molecular processes such as apoptosis. SPECT, PET, and MRI have been used to image angiogenesis and MMP activity. SPECT-CT has been used to localize FXIII activity in the infarct. Thus, a significant body of work sampling the full spectrum of infarct healing biology has been developed and applied in the preclinical setting. Building on this, a tremendous number of opportunities now exist in preclinical research to apply these methods to noninvasively and serially study disease progression and to evaluate potential new therapies. Also, there remain vast opportunities to develop imaging of additional important cellular and molecular targets. Importantly, while preclinical work continues to undergo steady progress, the translation of preclinical molecular imaging in infarct healing to clinical imaging of humans remains a major challenge.

The present review included examples from MRI, PET, and SPECT/SPECT-CT. While an ideal imaging examination would include assessment of cellular and molecular targets as well as imaging of anatomy, function, perfusion, and viability, no single modality is ideal, and all modalities have advantages and disadvantages (Table 2). Thus, hybrid imaging systems (such as SPECT-CT) or fusion of images from different modalities will probably offer the most rational approach when multimodal information is required. SPECT-CT and PET-CT systems are already successful, and MR-PET may soon be a clinical reality. These systems will likely be critical to the translation and success of clinical molecular imaging.

In conclusion, molecular imaging has remarkable potential to contribute to the management of patients recovering from acute MI by improving our understanding of disease processes and therapeutic mechanisms. The targeted molecular imaging approaches outlined in this review offer the potential to evaluate new therapies directed at infarct healing, regeneration, and repair. Furthermore, these new imaging methods might lead to more personalized care of patients after MI. There are many expectations for molecular imaging of infarct healing, and the task of translating experimental techniques into clinical practice is the greatest challenge for the coming years.

Acknowledgments Drs. Leor and Epstein acknowledge support from US-Israel Binational Science Foundation Grant 2007290. Dr. Epstein is also supported by NIH NIBIB R01 EB001763.

Disclosure No potential conflicts of interest relevant to this article were reported.

References

Papers of particular interest, published recently, have been highlighted as:
- Of importance

1. Lloyd-Jones D, Adams RJ, Brown TM et al.: Heart disease and stroke statistics—2010 update: a report from the American Heart Association. Circulation 2010, 121(7): e46–e215.
2. Leor J, Amsalem Y, Cohen S: Cells, scaffolds, and molecules for myocardial tissue engineering. Pharmacol Ther 2005, 105(2): 151–63.
3. Frangogiannis NG: The immune system and cardiac repair. Pharmacol Res 2008, 58(2): 88–111.
4. Nahrendorf M, Pittet MJ, Swirski FK: Monocytes: protagonists of infarct inflammation and repair after myocardial infarction. Circulation 2010, 121(22): 2437–45.
5. Frantz S, Bauersachs J, Ertl G: Post-infarct remodelling: contribution of wound healing and inflammation. Cardiovasc Res 2009, 81(3): 474–81.
6. Mann DL, Bogaev R, Buckberg GD: Cardiac remodelling and myocardial recovery: lost in translation? Eur J Heart Fail 2010, 12 (8): 789–96.
7. Shah AM, Solomon SD: A unified view of ventricular remodelling. Eur J Heart Fail 2010, 12(8): 779–81.
8. Frey B, Gaipl US: The immune functions of phosphatidylserine in membranes of dying cells and microvesicles. Semin Immunopathol 2010.
9. Fonge H, de Saint HM, Vunckx K et al.: Preliminary in vivo evaluation of a novel ^{99m}Tc-labeled HYNIC-cys-annexin A5 as an apoptosis imaging agent. Bioorg Med Chem Lett 2008, 18(13): 3794–8.
10. Hofstra L, Liem IH, Dumont EA et al.: Visualisation of cell death in vivo in patients with acute myocardial infarction. Lancet 2000, 356(9225): 209–12.
11. Sarda-Mantel L, Michel JB, Rouzet F et al.: (99 m)Tc-annexin V and (111)In-antimyosin antibody uptake in experimental myocardial infarction in rats. Eur J Nucl Med Mol Imaging 2006, 33(3): 239–45.
12. Dumont EA, Reutelingsperger CP, Smits JF et al.: Real-time imaging of apoptotic cell-membrane changes at the single-cell level in the beating murine heart. Nat Med 2001, 7(12): 1352–5.
13. Sosnovik DE, Schellenberger EA, Nahrendorf M et al.: Magnetic resonance imaging of cardiomyocyte apoptosis with a novel magneto-optical nanoparticle. Magn Reson Med 2005, 54(3): 718–24.
14. Fang W, Wang F, Ji S et al.: SPECT imaging of myocardial infarction using ^{99m}Tc-labeled C2A domain of synaptotagmin I in

a porcine ischemia-reperfusion model. Nucl Med Biol 2007, 34 (8): 917–23.
15. Zhao M, Li Z, Bugenhagen S: ^{99m}Tc-labeled duramycin as a novel phosphatidylethanolamine-binding molecular probe. J Nucl Med 2008, 49(8): 1345–52.
16. • Sarda-Mantel L, Hervatin F, Michel JB et al.: Myocardial uptake of ^{99m}Tc-annexin-V and ^{111}In-antimyosin-antibodies after ischemia-reperfusion in rats. Eur J Nucl Med Mol Imaging 2008, 35(1): 158-65. *This article describes the time course of apoptosis and necrosis using SPECT.*
17. • Sosnovik DE, Garanger E, Aikawa E et al.: Molecular MRI of cardiomyocyte apoptosis with simultaneous delayed-enhancement MRI distinguishes apoptotic and necrotic myocytes in vivo: potential for midmyocardial salvage in acute ischemia. Circ Cardiovasc Imaging 2009, 2(6): 460-7. *This article describes a novel method to image apoptosis and necrosis post-MI in vivo using MRI.*
18. Sosnovik DE, Nahrendorf M, Deliolanis N et al.: Fluorescence tomography and magnetic resonance imaging of myocardial macrophage infiltration in infarcted myocardium in vivo. Circulation 2007, 115(11): 1384–91.
19. Flogel U, Ding Z, Hardung H et al.: In vivo monitoring of inflammation after cardiac and cerebral ischemia by fluorine magnetic resonance imaging. Circulation 2008, 118(2): 140–8.
20. Leor J, Rozen L, Zuloff-Shani A et al.: Ex vivo activated human macrophages improve healing, remodeling, and function of the infarcted heart. Circulation 2006, 114(1 Suppl): I94–100.
21. • Montet-Abou K, Daire JL, Hyacinthe JN et al.: In vivo labelling of resting monocytes in the reticuloendothelial system with fluorescent iron oxide nanoparticles prior to injury reveals that they are mobilized to infarcted myocardium. Eur Heart J 2010, 31 (11): 1410-20. *This article demonstrates using MRI with iron-oxide particles to assess the infiltration of monocytes in MI. The monocytes were labeled prior to MI.*
22. Yang Y, Yang Y, Yanasak N, Schumacher A, Hu TC: Temporal and noninvasive monitoring of inflammatory-cell infiltration to myocardial infarction sites using micrometer-sized iron oxide particles. Magn Reson Med 2010, 63(1): 33–40.
23. Yang F, Liu YH, Yang XP, Xu J, Kapke A, Carretero OA: Myocardial infarction and cardiac remodelling in mice. Exp Physiol 2002, 87(5): 547–55.
24. Vandervelde S, van Amerongen MJ, Tio RA, Petersen AH, van Luyn MJ, Harmsen MC: Increased inflammatory response and neovascularization in reperfused vs. non-reperfused murine myocardial infarction. Cardiovasc Pathol 2006, 15(2): 83-90
25. Naresh NK, Vandsburger MH, Klibanov AL et al. Serial Quantitative Cellular MRI of Macrophage Infiltration in the Post-Infarct Heart Using T_1-Mapping and Gd-Liposomes [Abstract]. Circulation 2010, In press.
26. Xu Y, Klibanov AL, Beyers RJ et al.: Abstract 3364: Serial MRI Assessment of Macrophage Activity in the Murine Heart after Myocardial Infarction using Gadolinium-labeled Liposomes as a Positive Contrast Agent. Circulation 2007, 116(16_MeetingAbstracts): II.
27. Nahrendorf M, Swirski FK, Aikawa E et al.: The healing myocardium sequentially mobilizes two monocyte subsets with divergent and complementary functions. J Exp Med 2007, 204 (12): 3037–47.
28. • Panizzi P, Swirski FK, Figueiredo JL et al.: Impaired infarct healing in atherosclerotic mice with Ly-6C(hi) monocytosis. J Am Coll Cardiol 2010, 55(15): 1629-38. *This study presents a method to selectively image Ly-6C^{high} macrophages using FMT and also describes the effects of Ly-6C^{high} macrophages on infarct healing and post-MI remodeling.*
29. • Nahrendorf M, Sosnovik D, Chen JW et al.: Activatable magnetic resonance imaging agent reports myeloperoxidase activity in healing infarcts and noninvasively detects the antiinflammatory effects of atorvastatin on ischemia-reperfusion injury. Circulation 2008, 117 (9): 1153–60. *This article demonstrates the time course of myeloperoxidase post-MI in vivo using serial MRI.*
30. Heymans S, Luttun A, Nuyens D et al.: Inhibition of plasminogen activators or matrix metalloproteinases prevents cardiac rupture but impairs therapeutic angiogenesis and causes cardiac failure. Nat Med 1999, 5(10): 1135–42.
31. Vasilyev N, Williams T, Brennan ML et al.: Myeloperoxidase-generated oxidants modulate left ventricular remodeling but not infarct size after myocardial infarction. Circulation 2005, 112(18): 2812–20.
32. Meoli DF, Sadeghi MM, Krassilnikova S et al.: Noninvasive imaging of myocardial angiogenesis following experimental myocardial infarction. J Clin Invest 2004, 113(12): 1684–91.
33. • Higuchi T, Bengel FM, Seidl S et al.: Assessment of alphavbeta3 integrin expression after myocardial infarction by positron emission tomography. Cardiovasc Res 2008, 78(2): 395–403. *This article presents a novel technique to perform targeted imaging of the $\alpha_v\beta_3$ integrin to assess the time course of post-MI angiogenesis using PET.*
34. • Rodriguez-Porcel M, Cai W, Gheysens O et al.: Imaging of VEGF receptor in a rat myocardial infarction model using PET. J Nucl Med 2008, 49(4): 667-73. *This article describes imaging post-MI angiogenesis by PET with targeting VEGF.*
35. Dimastromatteo J, Riou LM, Ahmadi M et al.: In vivo molecular imaging of myocardial angiogenesis using the alpha(v)beta3 integrin-targeted tracer ^{99m}Tc-RAFT-RGD. J Nucl Cardiol 2010, 17(3): 435–43.
36. • Dobrucki LW, Tsutsumi Y, Kalinowski L et al.: Analysis of angiogenesis induced by local IGF-1 expression after myocardial infarction using microSPECT-CT imaging. J Mol Cell Cardiol 2010, 48(6): 1071-9. *This article details the application of targeted SPECT imaging of α_v integrins for studying the role of IGF-1 in infarct healing and LV remodeling.*
37. Oostendorp M, Douma K, Wagenaar A et al.: Molecular magnetic resonance imaging of myocardial angiogenesis after acute myocardial infarction. Circulation 2010, 121(6): 775–83.
38. Dobaczewski M, Gonzalez-Quesada C, Frangogiannis NG: The extracellular matrix as a modulator of the inflammatory and reparative response following myocardial infarction. J Mol Cell Cardiol 2010, 48(3): 504–11.
39. Su H, Spinale FG, Dobrucki LW et al.: Noninvasive targeted imaging of matrix metalloproteinase activation in a murine model of postinfarction remodeling. Circulation 2005, 112(20): 3157–67.
40. Chen J, Tung CH, Allport JR, Chen S, Weissleder R, Huang PL: Near-infrared fluorescent imaging of matrix metalloproteinase activity after myocardial infarction. Circulation 2005, 111(14): 1800–5.
41. • Helm PA, Caravan P, French BA et al.: Postinfarction myocardial scarring in mice: molecular MR imaging with use of a collagen-targeting contrast agent. Radiology 2008, 247(3): 788–96. *This article presents molecular MRI of myocardial scar post-MI using a collagen-targeting contrast agent.*
42. Caravan P, Das B, Dumas S et al.: Collagen-targeted MRI contrast agent for molecular imaging of fibrosis. Angew Chem Int Ed Engl 2007, 46(43): 8171–3.
43. Muzard J, Sarda-Mantel L, Loyau S et al.: Non-invasive molecular imaging of fibrosis using a collagen-targeted peptidomimetic of the platelet collagen receptor glycoprotein VI. PLoS One 2009, 4(5): e5585.
44. • Odaka K, Uehara T, Arano Y et al.: Noninvasive detection of cardiac repair after acute myocardial infarction in rats by ^{111}In Fab fragment of monoclonal antibody specific for tenascin-C. Int Heart J 2008, 49(4): 481-92. *This article demonstrates targeted SPECT imaging of tenascin-C post-MI.*

45. Taki J, Inaki A, Wakabayashi H et al.: Dynamic expression of tenascin-C after myocardial ischemia and reperfusion: assessment by ^{125}I-anti-tenascin-C antibody imaging. J Nucl Med 2010, 51 (7): 1116–22.
46. van den Borne SW, Isobe S, Verjans JW et al.: Molecular imaging of interstitial alterations in remodeling myocardium after myocardial infarction. J Am Coll Cardiol 2008, 52(24): 2017–28.
47. Nahrendorf M, Hu K, Frantz S et al.: Factor XIII deficiency causes cardiac rupture, impairs wound healing, and aggravates cardiac remodeling in mice with myocardial infarction. Circulation 2006, 113(9): 1196–202.
48. • Nahrendorf M, Aikawa E, Figueiredo JL et al.: Transglutaminase activity in acute infarcts predicts healing outcome and left ventricular remodelling: implications for FXIII therapy and antithrombin use in myocardial infarction. Eur Heart J 2008, 29(4): 445-54. *This article demonstrates the effects of FXIII on infarct healing and LV remodeling in vivo using SPECT-CT.*
49. Jugdutt BI: Limiting fibrosis after myocardial infarction. N Engl J Med 2009, 360(15): 1567–9.